

## Mineralogical Characterization of the Biodegradation of Sewage Cementitious Materials in the Presence of H<sub>2</sub>S

Janette Ayoub<sup>1</sup>, Tony Pons<sup>1</sup>, Marielle Guéguen Minerbe<sup>1</sup>, Marcos Oliveira<sup>2</sup> and Mario Marchetti<sup>3</sup>

<sup>1</sup>Univ. Gustave Eiffel, MAST-CPDM, F77454 Marne-la-Vallée, France,

[janette.ayoub@univ-eiffel.fr](mailto:janette.ayoub@univ-eiffel.fr), [tony.pons@univ-eiffel.fr](mailto:tony.pons@univ-eiffel.fr), [marielle.gueguen@univ-eiffel.fr](mailto:marielle.gueguen@univ-eiffel.fr)

<sup>2</sup>SIAAP- Direction Innovation, 82 avenue Kléber, 92700 Colombes, France, [marcos.oliveira@siaap.fr](mailto:marcos.oliveira@siaap.fr)

<sup>3</sup>Univ. Gustave Eiffel-Cerema, MAST-MCD, F77454 Marne-la-Vallée, France,

[mario.marchetti@univ-eiffel.fr](mailto:mario.marchetti@univ-eiffel.fr)

**Abstract.** *The biodegradation of cementitious materials in sewage systems is mainly due to the biotic oxidation of hydrogen sulfide (H<sub>2</sub>S) into sulfuric acid. It leads to a local and progressive dissolution of the cementitious matrix as well as the precipitation of some expansive products such as gypsum and ettringite. In such a context, this paper focuses on the characterization of the altered layers present on several types of cementitious materials (CEM I ordinary Portland cement, CEM III blast furnace cement, CEM V composite cement, and CAC: calcium aluminate cement). The studied samples are mortars exposed, to different H<sub>2</sub>S concentrations, for several years in a local sewage plant managed by the Interdepartmental Syndicate for the Sanitation of the Paris Agglomeration (SIAAP). Transversal cross-sections of these mortars were first chemically characterized by energy dispersive spectroscopy (EDS) in order to obtain elemental mapping. Additionally, to better understand the surface degradation and the appearance of mineral phases revealing the process,  $\mu$ -Raman mappings were performed on the deteriorated zones at different time scales. Gypsum was observed on all samples. The analysis confirmed the greater resistance of CAC materials in such an environment than that of Portland cement-based materials.*

**Keywords:** *Biodegradation; Cementitious materials; Sewage systems; SEM;  $\mu$ -Raman.*

### 1 Introduction

As part of the process of building a more sustainable world, the United Nations have defined its sixth sustainable development goal, to ensure access to water and sanitation for everyone by 2030 and to ensure sustainable management of water resources (Bodiguel, s. d.). In this regard, a key action leads professionals in the sanitation sector to examine the construction of sustainable networks and the optimal management methods to be implemented for these structures.

Among the available pipe materials, cementitious materials are the most widely utilized and account for about half of the quantity of large diameter sewer pipes. However, during their lifetime, these pipes are undergoing various types of deterioration. These deteriorations can be related to a defect during assembly, to environmental aggression or to deterioration by effluents and micro-organisms circulating inside the pipe. About 40% of these deteriorations can be attributed to biogenic attack via sulfuric acid production (Kaempfer & Berndt, 1999). The different stages of the phenomenon encountered during this biodegradation can be found in the literature by Aboulela; Grandclerc; Herisson et Okabe et al. (Aboulela, 2022; Grandclerc, 2017; Herisson, 2012; Okabe et al., 2007).

However, the biodeterioration of cementitious materials in the presence of  $H_2S$ , can be summarized by four steps: an abiotic oxidation of  $H_2S$  to elemental sulfur on the surface of the cementitious material; a bacterial oxidation of sulfur-containing molecules to sulfuric acid; a sulfuric acid diffusion into the degraded layer; and an acid attack on intact cementitious materials (Herisson et al., 2013).

Sulfuric acid dissolves the cementitious matrix and leads to the formation of non-cohesive and/or expansive sulfate mineral products such as gypsum and ettringite (Herisson et al., 2017). The durability of cementitious materials exposed to such conditions is highly dependent on the nature of the binder. The literature presents different in-situ studies that investigate and compare the resistance of several cementitious materials to biodeterioration. These studies show in particular the better resistance of calcium aluminate cement (CAC) to biodeterioration compared to Portland cement (Herisson, 2012). (Grandclerc et al., 2018) have also reported that, among the different Portland cements, CEM V has a better resistance than CEM III and CEM I.

The objective of this work is to study the behavior of different mortar formulations and to provide a mineralogical characterization of the deterioration layers present on these different types of cementitious binders. So, the mortars were exposed for four years in-situ with a periodic macroscopic follow-up. Furthermore, as Raman spectroscopy is a high spatial resolution and non-destructive technique (Kong et al., 2011), it was used to characterize certain phases and better understand the biodeterioration process.

## **2 Experimental Procedures**

### **2.1 Mortar Samples**

Cylindrical mortar samples of 6 cm diameter and 14 cm height were prepared with four types of cement (ordinary Portland cement: CEM I, blast furnace cement: CEM III, slag and ash compound cement: CEM V, and calcium aluminate cement: CAC). The water/cement ratio and sand/cement ratio are 0.5 and 0.3 respectively for all samples. A PVC tube was inserted in the center of each sample in order to fix each one in a  $60 \times 40 \times 30 \text{ cm}^3$  box which was later placed in the sewerage system and opened to the gas flow. After preparation, the samples were exposed to a relative humidity of 100% for 24 hours. Once unmolded, the samples were stored in sealed plastic bags for 28 days.

### **2.2 Characteristics of the Exposure Site**

The exposure site is located in the general outfall in the northern part of the Paris region where the samples were exposed for four years. They were then submitted to different  $H_2S$  concentrations. Throughout the exposure period, the  $H_2S$  concentration was measured at the site using a safety sensor. The variation in  $H_2S$  concentration for a 9-month period of the exposure duration is shown in the Figure 1. According to Table 1, the  $H_2S$  concentration in the gas phases varied from 0 ppm to a maximum of 598 ppm with an average concentration of 14 ppm (which corresponds to the exposure class XA3 according to the NF EN 206/CN (Iv, s. d.)). This concentration reached different levels and underwent several variations over two orders of magnitude.

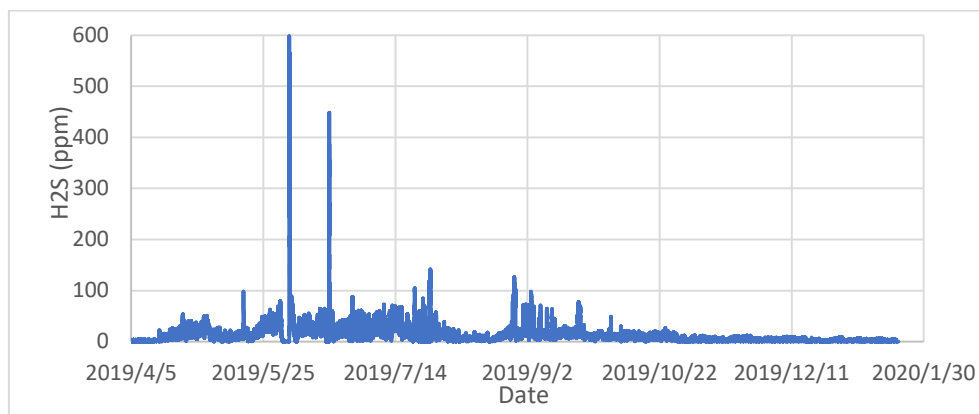


**Figure 1:** H<sub>2</sub>S concentration as a function of time over a 9-month duration.

**Table 1:** H<sub>2</sub>S concentration in ppm in the gas phase of the exposure site.

Mean (ppm)	14.00	1st quartile (ppm)	4	Min (ppm)	0
Standard deviation (ppm)	18.86	3rd quartile (ppm)	19	Max (ppm)	598

### 2.3 Analysis of Cementitious Samples

For each sampling time step, visual observations were first made on site to determine the macroscopic degradations of the mortar samples. Surface pH (pH paper with 0.2 accuracy), weights (scale with 0.1g accuracy), and diameters (caliper) were also measured on site. In addition, observations were made on a cross-section of each mortar with an optical-digital microscope (Keyence) that allowed the determination of the deteriorated zone thickness by image analysis using ImageJ software.

In order to follow up on the mineralogical characterizations of the samples, measurements were made using a BWTek iRaman spectrometer, with a laser at 532 nm (50 mW), with a spectral resolution of 4 cm<sup>-1</sup>. It was coupled to a microscope with a x50 objective.

The elemental chemical analyses of the metallized samples were performed using Scanning Electron Microscope (Quanta 400 FEI) equipped with an Energy Dispersive Spectrometer (EDS, Xplore30, Oxford), at 20kV.

## 3 Results

### 3.1 Visual Observations





















Macroscopic degradations of the samples were observed throughout the in-situ exposure in a qualitative (visual) manner as illustrated in Figure 2. For all samples, this degradation is present from the first observation (1.8 years) and it worsens with time. This degradation is accompanied by precipitation on the surface of the mortars and loss of material. Moreover, a change of color and a precipitation of gypsum (confirmed by DRX) are visible on all the samples.

CAC shows better resistance to biodeterioration with respect to Portland cement, which is consistent with the literature (Herisson, 2012). This observation is based on the fact that the CAC sample retained its geometric characteristics, while the CEM I sample showed signs of

geometric change.

CEM I appears to be the most degraded formulation. As well, an alteration of the angles is observed for CEM I, CEM III and CEM V after 2.2 years.

However, according to the literature (Grandclerc et al., 2018), CEM III should have behaved differently than what was visually observed in this study and should have exhibited greater degradation.

Cement	Reference	1.8 years	2.2 years	2.8 years	4 years
CEM I					
CEM III					
CEM V					
CAC					

**Figure 2:** Visual observations of the mortars during the 4 years of exposure.

### 3.2 Evolution of Surface pH, Weights and Diameter of Mortar Samples

Besides the visual degradation, the surface pH, masses and diameters of the samples were measured during the in-situ exposure period. The surface pH decreased sharply from its initial alkaline value after 1.8 years and then stabilized between 4 and 6 with the years, as shown in Figure 3-a. Along with the pH evolution, a weight gain is also observed. This gain is obviously

related to water accumulation in the mortar pores, present in all samples during the first years as shown in Figure 3-b. Then, a weight loss is observed for the CEM I, CEM III and CEM V samples between the 2nd and 4th year while the one of CAC seems to remain constant. Finally, the evolution of the diameter of the samples is shown in Figure 3-c. This one showed the same behavior as the mass, with a variation after 2.8 years during which a strong precipitation of gypsum was observed on the samples, leading to an increase in their diameter. A significant difference in thickness increase between CEM I and CEM V and the other formulations after 2.8 years of exposure was noticed. In contrast, no significant change in diameter was measured for CAC mortars. These measurements are consistent with the visual observations.

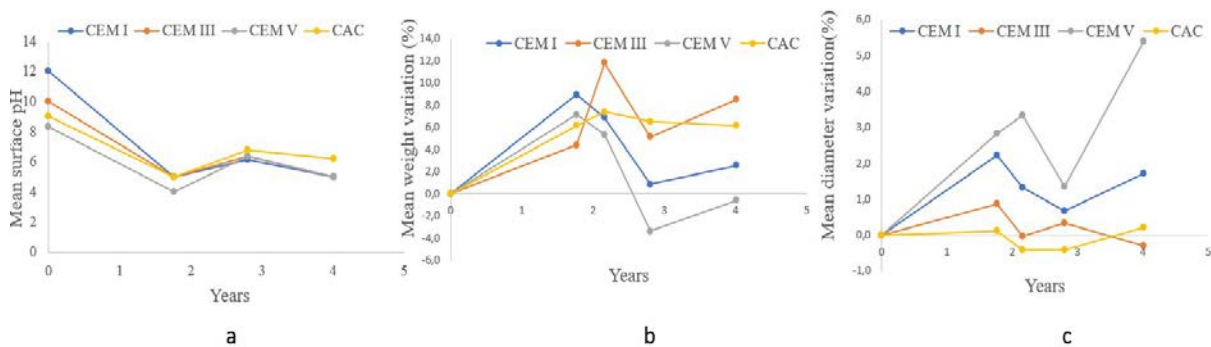


**Figure 3:** Mean measurements from 0 to 4 years of (a) surface pH, (b) masses, and (c) diameter of samples.

### 3.3 Determination of Visual Degraded Thicknesses.

The cross-sections of the mortars after four years of exposure in the sewer system, observed with an optical-digital microscope in reflected light, are shown in Figure 4. They confirm the results presented in the previous section. Figure 4-a and 4-b clearly show the annular progression of degradation for CEM I and CEM V mortars, and less marked for CAC sample (Figure 4-c). Figure 4-c confirms the greater resistance of CAC as its degradation layer thickness is smaller than those of Portland cements.

In addition, these cross-sections allowed us to distinguish the degraded mortar zones from the pristine ones. At the interface of these two zones, an orange/brown layer is visible, probably related to the presence of iron (Grengg et al., 2017). All of these observations made possible to quantitatively determine the thicknesses of the degraded, chemically altered, and healthy zones (Figure 5) of the mortars using ImageJ software (Table 2). These values support the results in Figure 3-b and 3-c, showing that the radius of CEM I and CEM V increased after four years (Table 2).

**Table 2:** Quantitative determination of the thicknesses of the degraded, altered and intact zones.

Cement	Initial radius (r1: cm)	Radius at t=4 years (r2: cm)	Radius of pristine zone (r3: cm)	Mean visual modified thickness after 4 years (cm)
CEM I	3.00	3.03	1.93	1.07
CEM V	3.00	3.11	2.39	0.61
CAC	3.00	2.97	2.95	0.05

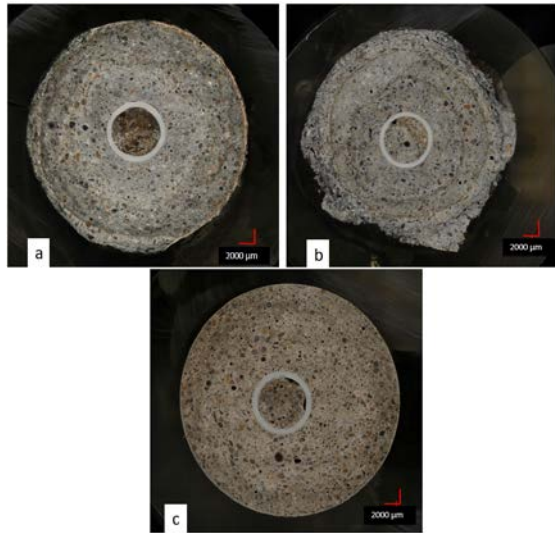


**Figure 4:** Cross section of mortars observed with KEYENCE (a) CEM I, (b) CEM V, (c) CAC after four years of exposure in a sewer system

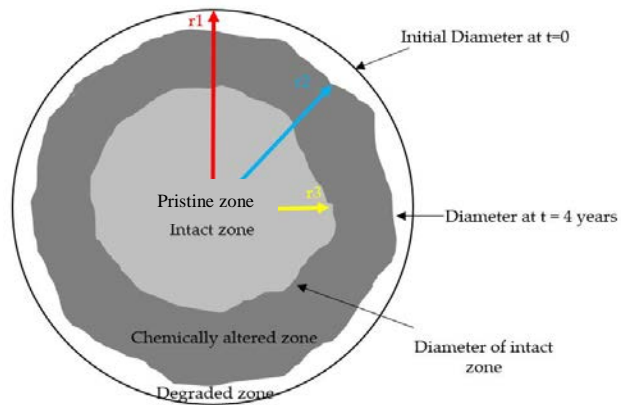


**Figure 5:** Schematic of the degraded, chemically altered and intact zone of a sample.

### 3.4 Mineralogical Characterizations by $\mu$ -Raman Spectroscopy

The photographs of the intact and altered zones (Figure 6-a and 6-b respectively) of polished sections of a CEM I specimen (with cement paste and aggregates) show significant morphological differences. Furthermore, the spectral analysis (Raman at 532 nm, integration time 40 s, average over 20 spectra, x50 objective) of the altered zone highlights a typical gypsum spectrum at  $1008\text{ cm}^{-1}$ , obtained in the CEM I specimen (see Figure 6-c). It is essential to note that the observed vibrational modes are in good agreement with literature data (Chang et al., 1999; Pons et al., 2018; Tang et al., 2021), with in particular the intense peak at  $1008\text{ cm}^{-1}$  characteristic of gypsum, formed after sulfate attack. On the other hand, the spectral analysis of the sound zone shows the spectral signature of cement as found in the literature with the presence of amorphous structures (Marchetti et al., 2023), and shows no significant or characteristic peak of anhydrous or hydrated calcium sulfate. These elements confirm the relevance of the spectroscopic approach to characterize the bio-alteration of the cement matrix.

### 3.5 Chemical Observations

Some results of the chemical observation by SEM-EDS of a mapping of a section of a CEM I sample are presented in Figure 7. This cartography allows us to clearly distinguish the degraded zone from the non-degraded one (Figure 7-a). The results of the elemental iron mapping are consistent with the observations previously described in Section 3.3. This orange/brown layer, visible at the interface of the two zones, is related to the presence of iron (Figure 7-b). Moreover, the outer part of the deteriorated layer was featured by alternating S and Ca filaments (Figure 7-c and 7-d respectively), corresponding to sulfate salts as gypsum, in conformity with the Raman spectroscopy results.



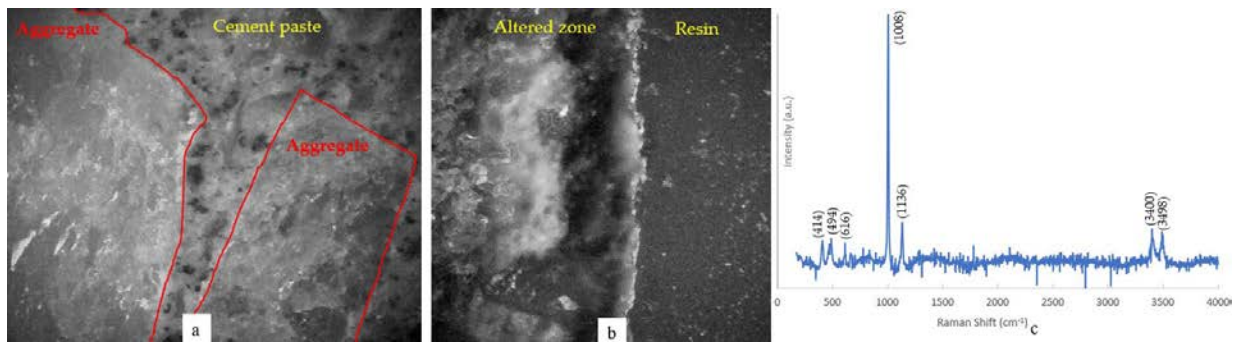


**Figure 6:** Photographs (in reflected light) of an intact zone (a) and an altered one (b) and normalized Raman spectra of the periphery (c) of polished sections of a CEM I specimen after four years of exposure in a sewage system.

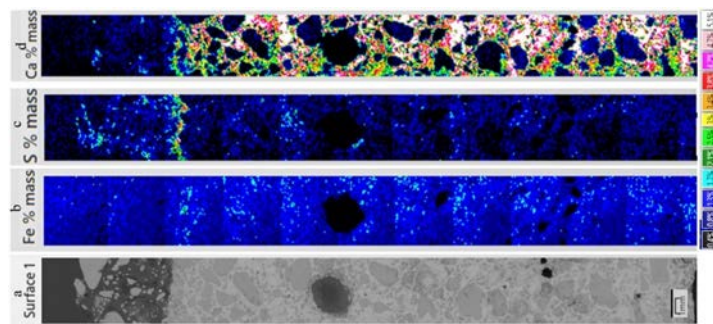


**Figure 7:** SEM-EDS mapping of CEM I cement-based mortars from the deteriorated zone (top part) to the intact zone (bottom part) (a), with the associated mapping for iron (b), sulfur (c) and calcium (d).

## 4 Conclusion

In this study, the macroscopic behavior of different mortar formulations with respect to bio-alteration in a  $H_2S$ -enriched environment was investigated. The evolution of macroscopic parameters such as visual aspect, surface pH, mass and diameter of the mortars, was followed during four years of exposure. The alteration layers present on these different types of cementitious binders were characterized by different analytical techniques. The results of this study allowed to classify the materials from the most to the least resistant as follows: CAC, CEM V, CEM I. All these results are consistent with the literature (Grandclerc, 2017; Herisson, 2012). Furthermore, the better resistance of CAC mortars among all formulations is attributed to the chemical stability of the  $AH_3$  phase which upon dissolution releases hydroxyl ions that neutralize the acid and thus increases the pH by destabilizing the "optimal" acid medium for biogenic sulfuric acid production (Aboulela, 2022; Buvignier, 2018). However, the study of chemical and mineralogical variations, using scanning electron microscopy along with  $\mu$ -Raman spectroscopy, confirmed the observations and findings of the literature, while opening more possibilities on the quantitative analysis of the degradation process (Grenng et al., 2017).

### Acknowledgements

This project has received funding from the European Union's Horizon 2020 research and innovation programme under the Marie Skłodowska-Curie COFUND grant agreement No 101034248.



Funded by  
the European Union

## References

- Aboulela, A. (2022). Study of the resistance to biodeterioration of innovative low-carbon cementitious materials for application in sewer networks.
- Bodiguel, J. (s. d.). Développement Durable : Garantir l'accès de tous à l'eau. Développement durable. Consulté 10 janvier 2023, à l'adresse <https://www.un.org/sustainabledevelopment/fr/water-and-sanitation/>
- Buvignier, A. (2018). Caractérisation du rôle de l'aluminium dans les interactions entre les microorganismes et les matériaux cimentaires dans le cadre des réseaux d'assainissement.
- Chang, H., Huang, P. J., & Hou, S. C. (1999). Application of thermo-Raman spectroscopy to study dehydration of  $\text{CaSO}_4 \cdot 2\text{H}_2\text{O}$  and  $\text{CaSO}_4 \cdot 0.5\text{H}_2\text{O}$ . *Materials Chemistry and Physics*.
- Grandclerc, A. (2017). Compréhension des mécanismes de biodétérioration des matériaux cimentaires dans les réseaux d'assainissement : Étude expérimentale et modélisation.
- Grandclerc, A., Guéguen-Minerbe, M., & Chaussadent, T. (2018). Accelerated biodeterioration test of cementitious materials in sewer networks.
- Grengg, C., Mittermayr, F., Koraimann, G., Konrad, F., Szabó, M., Demeny, A., & Dietzel, M. (2017). The decisive role of acidophilic bacteria in concrete sewer networks : A new model for fast progressing microbial concrete corrosion. *Cement and Concrete Research*, 101, 93-101. <https://doi.org/10.1016/j.cemconres.2017.08.020>
- Herisson, J. (2012). Biodétérioration des matériaux cimentaires dans les ouvrages d'assainissement : Étude comparative du ciment d'aluminate de calcium et du ciment Portland.
- Herisson, J., Guéguen-Minerbe, M., van Hullebusch, E. D., & Chaussadent, T. (2017). Influence of the binder on the behaviour of mortars exposed to  $\text{H}_2\text{S}$  in sewer networks : A long-term durability study. *Materials and Structures*, 50(1), 8. <https://doi.org/10.1617/s11527-016-0919-0>
- Herisson, J., van Hullebusch, E. D., Moletta-Denat, M., Taquet, P., & Chaussadent, T. (2013). Toward an accelerated biodeterioration test to understand the behavior of Portland and calcium aluminate cementitious materials in sewer networks. *International Biodeterioration & Biodegradation*, 84, 236-243. <https://doi.org/10.1016/j.ibiod.2012.03.007>
- Iv, C. (s. d.). Sommaire du fascicule FD P 18-01.
- Kaempfer, W., & Berndt, M. (1999). Estimation of service life of concrete pipes in sewer networks. *Durability of Building Materials and Components* 8.
- Kong, C.-R., Barman, I., Dingari, N. C., Kang, J. W., Galindo, L., Dasari, R. R., & Feld, M. S. (2011). A novel non-imaging optics based Raman spectroscopy device for transdermal blood analyte measurement. *AIP Advances*, 1(3), 032175. <https://doi.org/10.1063/1.3646524>
- Marchetti, M., Mechling, J.-M., Janvier-Badosa, S., & Offroy, M. (2023). Benefits of Chemometric and Raman Spectroscopy Applied to the Kinetics of Setting and Early Age Hydration of Cement Paste. *Applied Spectroscopy*, 77(1), 37-52. <https://doi.org/10.1177/00037028221135065>
- Okabe, S., Odagiri, M., Ito, T., & Satoh, H. (2007). Succession of Sulfur-Oxidizing Bacteria in the Microbial Community on Corroding Concrete in Sewer Systems. *Applied and Environmental Microbiology*, 73(3), 971-980. <https://doi.org/10.1128/AEM.02054-06>
- Pons, T., Fourdrin, C., Grandclerc, A., Gueguen-Minerbe, M., Tarrida, M., Lavigne, P., van Hullebusch, E., Chaussadent, T., & Pechaud, Y. (2018). Mineralogical characterization of the alteration layer of chemically and biologically altered cementitious materials.
- Tang, C., Ling, T.-C., & Mo, K. H. (2021). Raman spectroscopy as a tool to understand the mechanism of concrete durability—A review. *Construction and Building Materials*, 268, 121079. <https://doi.org/10.1016/j.conbuildmat.2020.121079>